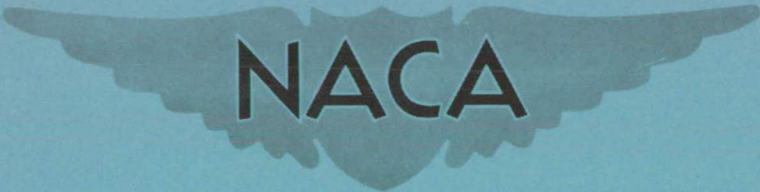


CONFIDENTIALCopy
RM L53E28a
NACA

RESEARCH MEMORANDUM

INVESTIGATION AT TRANSONIC SPEEDS OF THE HINGE-MOMENT AND
LIFT-EFFECTIVENESS CHARACTERISTICS OF A SINGLE FLAP
AND A TANDEM FLAP ON A 60° DELTA WING

By Delwin R. Croom and Harleth G. Wiley

Langley Aeronautical Laboratory
Langley Field, Va.

CLASSIFICATION CHANGED TO UNCLASSIFIED

AUTHORITY J.W. CROWLEY DATE: 10-12-54

CHANGE NO. 2787

WHL

CLASSIFIED DOCUMENT

This material contains information affecting the National Defense of the United States within the meaning of the espionage laws, Title 18, U.S.C., Secs. 793 and 794, the transmission or revelation of which in any manner to an unauthorized person is prohibited by law.

**NATIONAL ADVISORY COMMITTEE
FOR AERONAUTICS**

WASHINGTON

July 24, 1953

CONFIDENTIAL

NATIONAL ADVISORY COMMITTEE FOR AERONAUTICS

RESEARCH MEMORANDUM

INVESTIGATION AT TRANSONIC SPEEDS OF THE HINGE-MOMENT AND

LIFT-EFFECTIVENESS CHARACTERISTICS OF A SINGLE FLAP

AND A TANDEM FLAP ON A 60° DELTA WING

By Delwin R. Croom and Harleth G. Wiley

SUMMARY

An investigation was made in the Langley high-speed 7- by 10-foot tunnel by means of the transonic-bump technique to determine the hinge-moment and lift-effectiveness characteristics of a 0.67 semispan single flap and a 0.67 semispan tandem flap on a thin 60° delta wing. The wing was a flat plate with beveled leading and trailing edges and had a maximum thickness ratio of 0.045, 60° sweepback at the leading edge, and an aspect ratio of 2.31.

The results indicated that although the tandem flap had less variation of $C_{h\delta}$ (hinge-moment coefficient per degree flap deflection) with Mach number than did the single flap, the lift effectiveness was only approximately 50 percent of that obtained with the single flap.

INTRODUCTION

The use of airfoil surfaces in tandem to restrict the chordwise center-of-pressure travel with Mach number on control surfaces and thus reduce large hinge-moment-coefficient variations with Mach number was originally proposed and investigated in Germany, and the results were reported in reference 1. The German research consisted of wind-tunnel tests at subsonic and supersonic speeds on tandem-type controls of relatively thick sections with large trailing-edge angles. The results of the tests show about the same variation of hinge-moment coefficient with deflection in both the speed regimes. No data were presented in reference 1, however, of the effectiveness of the control nor were there any results at transonic speeds. In order to evaluate this type of control at transonic speeds, an investigation was made by means of the

transonic-bump technique in the Langley high-speed 7- by 10-foot tunnel to determine the comparative hinge-moment and lift-effectiveness parameters of a single flap and a tandem flap on a thin 60° delta wing. The constant-chord single flap was of double-wedge airfoil section hinged at the 87.3-percent wing-root-chord station and had a 46.2-percent-flap-chord overhang balance. The tandem flap was similar to the single flap in outside dimensions and consisted essentially of two double-wedge airfoil sections in tandem. The wing used in the investigation was a flat plate with beveled leading and trailing edges, a maximum thickness ratio of 0.045, 60° sweepback at the leading edge, and an aspect ratio of 2.31.

Lift and hinge-moment characteristics are presented for a range of Mach numbers of 0.60 to 1.11, an angle-of-attack range of -6° to 15°, and a flap-deflection range of ±20°.

COEFFICIENTS AND SYMBOLS

C_L	lift coefficient, $\frac{\text{Twice lift of semispan model}}{qS}$
C_h	flap hinge-moment coefficient, $H/q2M'$
H	flap hinge moment measured about hinge line, lb-ft
M'	area moment of single flap rearward of hinge line, 0.0010654 ft ³
q	effective dynamic pressure over span of model, $\rho V^2/2$, lb/sq ft
S	twice wing area of semispan model, sq ft
b	twice span of semispan model, ft
\bar{c}	mean aerodynamic chord of wing, $\frac{2}{S} \int_0^{b/2} c^2 dy$, 0.461 ft
c	local wing chord, ft
c_f	flap chord, (distance from hinge line rearward to wing trailing edge), ft

c_r	wing root chord, ft
y	semispan distance from plane of symmetry, ft
ρ	mass density of air, slugs/cu ft
V	free-stream air velocity, ft/sec
M	effective Mach number over span of model, $\frac{2}{S} \int_0^{b/2} cM_a dy$
M_a	average chordwise local Mach number
M_l	local Mach number
R	Reynolds number of wing based on \bar{c}
α	angle of attack of wing, deg
δ	flap deflection, measured perpendicular to flap hinge line (positive when flap trailing edge is down)

$$C_{L\delta} = \left(\frac{\partial C_L}{\partial \delta} \right)_{\alpha}$$

$$C_{h\delta} = \left(\frac{\partial C_h}{\partial \delta} \right)_{\alpha}$$

$$C_{h\alpha} = \left(\frac{\partial C_h}{\partial \alpha} \right)_{\delta}$$

The subscripts outside the parenthesis indicate the factor held constant during the measurement of the parameters.

MODEL AND APPARATUS

The steel semispan wing model used in this investigation had 60° sweepback of the leading edge, 0° sweep of the trailing edge, an aspect ratio of 2.31, and a taper ratio of 0 (fig. 1). The model was made of a flat steel plate, 1/8 inch thick, with beveled leading and trailing edges. The airfoil thickness varied from 1.5 percent chord

at the root to 4.5 percent chord at $0.67b/2$, and remained constant at 4.5 percent chord from $0.67b/2$ to the tip.

The wing was equipped with interchangeable single and tandem trailing-edge flaps extending from the wing root chord to $0.67b/2$. Each flap was hinged at the $0.873c_r$ line and had $0.462c_f$ overhang balance. The single flap had a double-wedge airfoil section and a constant chord of $0.127c_r$. The tandem flap was similar in outside dimensions to the single flap and consisted of two parallel double-wedge airfoil sections rigidly attached in tandem with $0.045c_r$ gap between them. The gap between the wing and flap was about $0.005c_f$ for both configurations and was unsealed. Flap hinge moments were measured by a calibrated beam-type electric strain gage fastened rigidly to a torsion rod below the bump surface.

The model was mounted on an electrical strain-gage balance which was enclosed within the bump. The balance chamber was sealed except for a small rectangular clearance hole in the bump turntable through which an extension of the wing butt passed. Air leakage through the hole was kept to a minimum by the use of a sponge-rubber wiper seal fastened to the undersurface of the bump turntable. Aerodynamic forces and moments were measured with calibrated potentiometers.

TESTS

The tests were made in the Langley high-speed 7- by 10-foot tunnel by utilizing the transonic-bump technique. This technique is described in reference 2 and involves the mounting of the model in the high-velocity flow field generated over the curved surface of a bump located on the tunnel floor.

Typical contours of local Mach number distribution in the vicinity of the model but with the model removed are shown in figure 2. The dashed line shown near the root chord indicates a local Mach number that is 5 percent below the effective test Mach number and represents the extent of the estimated boundary layer. The effective test Mach numbers were obtained from contour charts similar to those of figure 2 by using the relationship

$$M = \frac{2}{S} \int_0^{b/2} cM_a dy$$

The variation of Reynolds number with Mach number for typical test conditions is presented in figure 3. The Reynolds numbers were based on

a mean aerodynamic chord of 0.461 foot and varied from approximately 1,400,000 to 1,800,000.

Lift and hinge-moment data were obtained through a Mach number range of 0.60 to 1.11 and over an angle-of-attack range of -6° to 15° . The range of flap deflections tested varied from about $\pm 20^\circ$ at the low Mach numbers to about $\pm 7.5^\circ$ at the higher Mach numbers.

CORRECTIONS

No corrections have been applied to the data for the chordwise and spanwise Mach number gradients or for distortion of the wing due to aerodynamic loads, but these corrections are believed to be small. Flap-deflection corrections as applied were determined from a static hinge-moment calibration with torsion loads applied at the midspan of the flap. The maximum flap-deflection correction for the extreme loading condition was about 3.5° .

RESULTS AND DISCUSSION

The variations of lift coefficient with flap deflection for the single and tandem flaps are presented in figures 4 and 5, respectively. The variations of hinge-moment coefficient C_h with flap deflection δ for the single and tandem flaps are presented in figures 6 and 7, respectively. Cross plots of hinge-moment coefficient against angle of attack at $\delta = 0^\circ$, obtained from figures 6 and 7, are presented in figures 8 and 9 for the single and tandem flaps, respectively. (For the purpose of comparison of hinge moments; the hinge-moment coefficients for both flaps are based on the area moment rearward of the hinge line of the single flap.)

The variation of C_h with δ for both flaps was generally linear for $\pm 5^\circ$ flap deflection throughout the Mach number range. At approximately $\pm 7.5^\circ$ flap deflection, at Mach numbers up to 0.90, a reversal in trend of C_h with δ is evident for both flaps ($C_{h\delta}$ becomes positive in the vicinity of $\delta = \pm 7.5^\circ$ at the lower angles of attack up to a Mach number of 0.90). This reversal in trend is probably a function of the unporting of the sharp leading edge above the surface of the wing since both flaps unport at approximately 7.25° flap deflection.

The comparative effects of Mach number on the hinge-moment parameters $C_{h\delta}$ and $C_{h\alpha}$ and the lift-effectiveness parameter $C_{L\delta}$ are

shown in figure 10. The variation of $C_{h\delta}$ with Mach number of the tandem flap was less than that of the single flap which is in agreement with the results of reference 1 obtained at subsonic and supersonic speeds. At Mach numbers below 0.95, $C_{h\delta}$ is greater negatively for the tandem flap than for the single flap and at Mach numbers above 0.95 there is no appreciable difference in $C_{h\delta}$ for the two flaps. A larger variation of $C_{h\alpha}$ with Mach number was noted for the tandem flap than for the single flap. The lift effectiveness $C_{L\delta}$ of the tandem flap is approximately 50 percent of that obtained with the single flap throughout the Mach number range. These large losses of lift effectiveness of the tandem flap would in most cases outweigh the advantages of having less variation of $C_{h\delta}$ with Mach number.

CONCLUSIONS

On the basis of wind-tunnel tests of a single flap and a tandem flap on a 60° delta wing at transonic speeds, the following conclusions were reached:

1. The tandem flap had less variation of $C_{h\delta}$ (hinge-moment coefficient per degree flap deflection) with Mach number than the single flap and had greater values of $C_{h\delta}$ at subsonic speeds.
2. The tandem flap produced only about 50 percent as much lift effectiveness as was produced by the single flap.

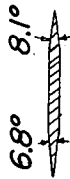
Langley Aeronautical Laboratory,
National Advisory Committee for Aeronautics,
Langley Field, Va., May 15, 1953.

REFERENCES

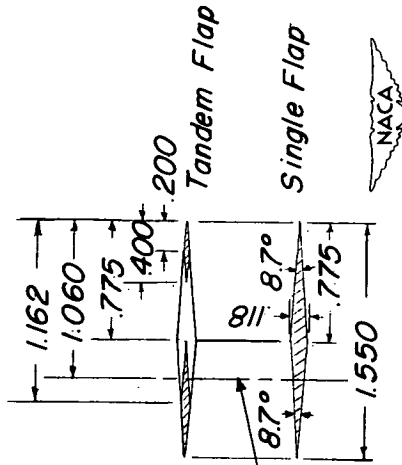
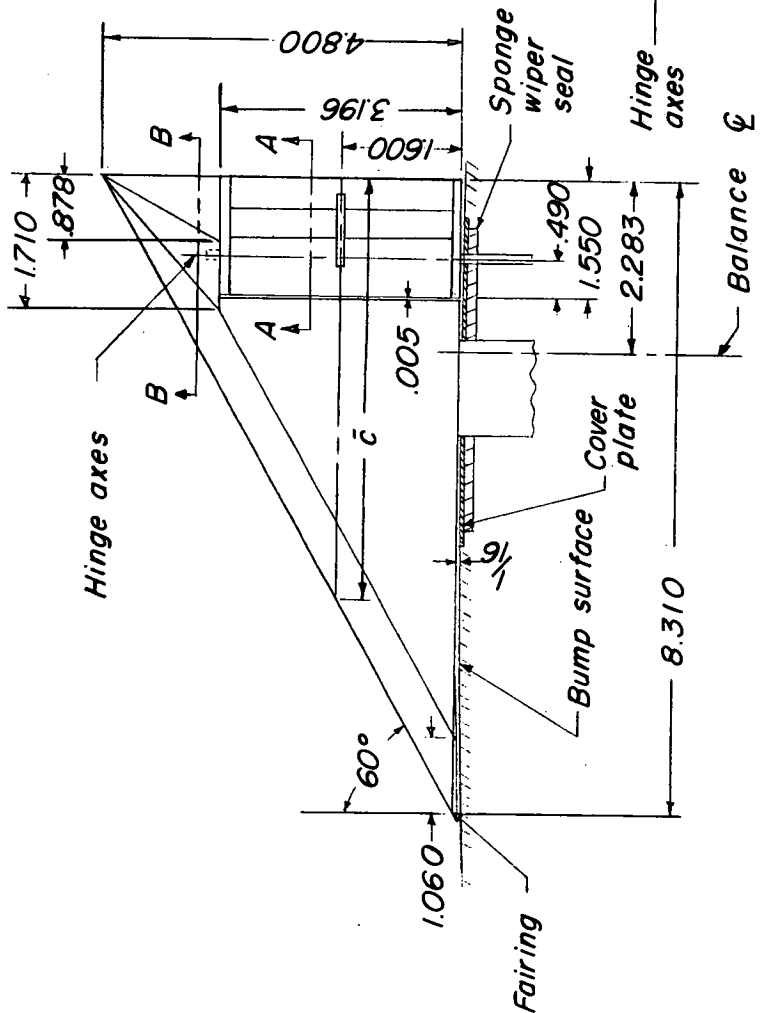
1. Wegener and Eckert: Ruderentwicklung im Windkanal zur Raketensteuerung im Unter- und Überschall. WVA Archiv Nr. 165, Wasserbau-Versuchsanstalt (München), Mar. 20, 1945.
2. Schneiter, Leslie E., and Ziff, Howard L.: Preliminary Investigation of Spoiler Lateral Control on a 42° Sweptback Wing at Transonic Speeds. NACA RM L7F19, 1947.

TABULATED WING DATA

Twice semispan area .277 sq ft
 Aspect ratio 2.31
 Taper ratio 0
 Mean aerodynamic chord 461 ft



Section B-B



Section A-A

Figure 1.- General arrangement of the model used in the investigation.
 All dimensions are in inches unless otherwise noted.

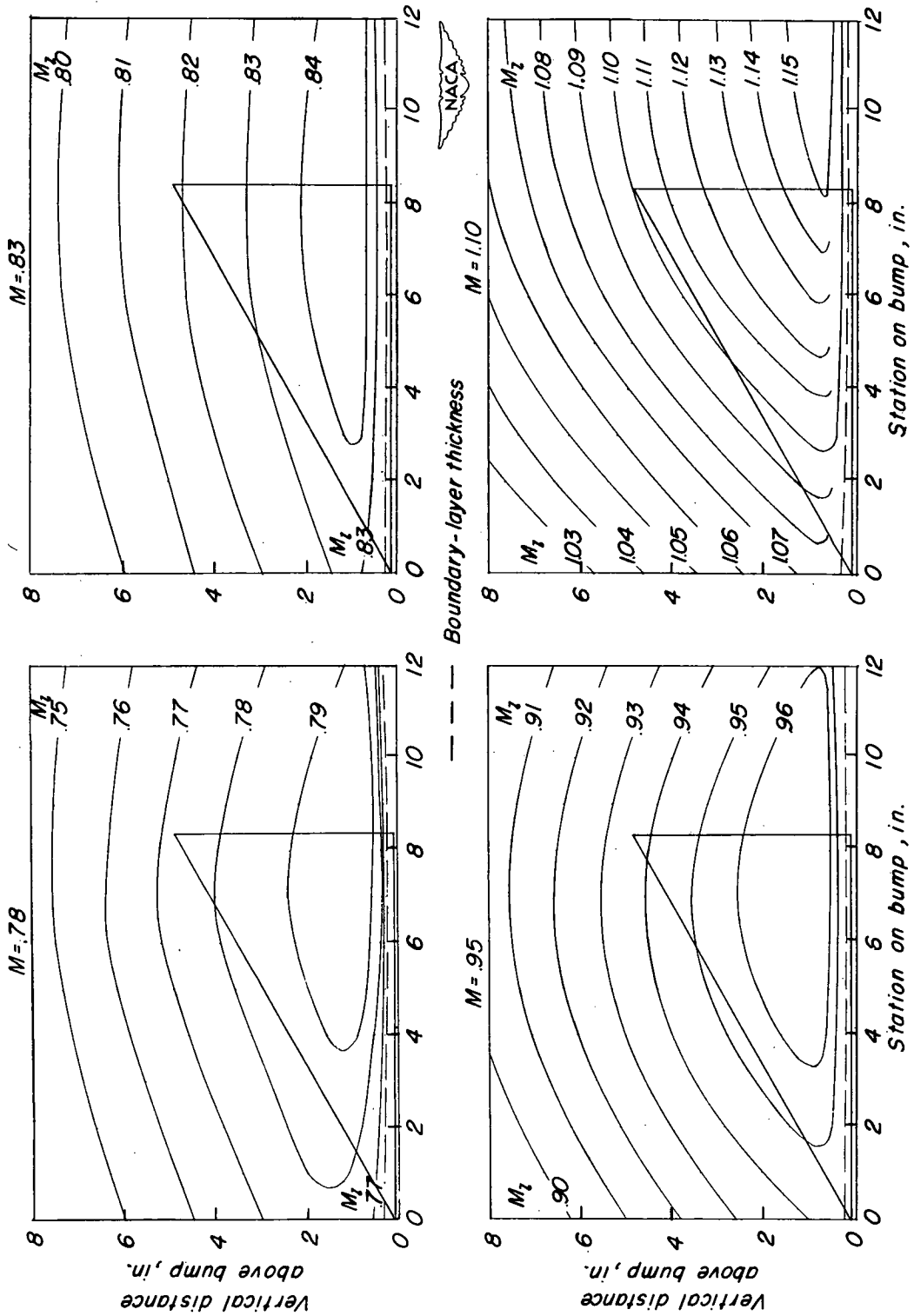


Figure 2.- Typical Mach number contours over transonic bump in region of model location.

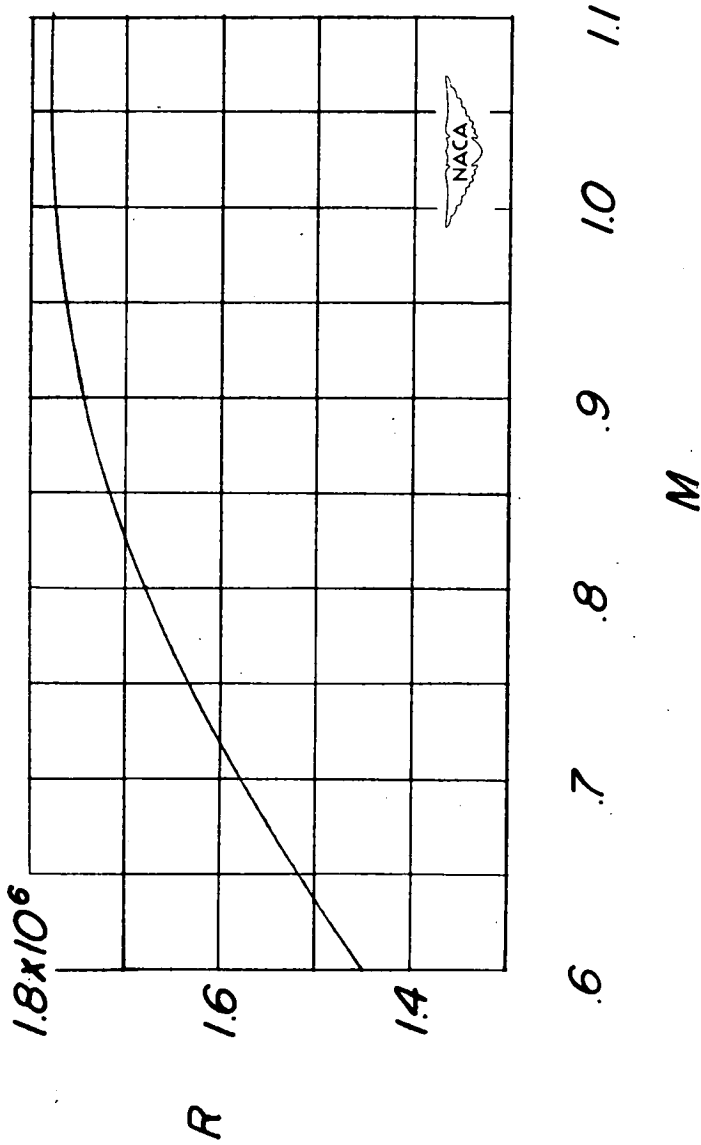


Figure 3.- Typical variation of test Reynolds number with Mach number.

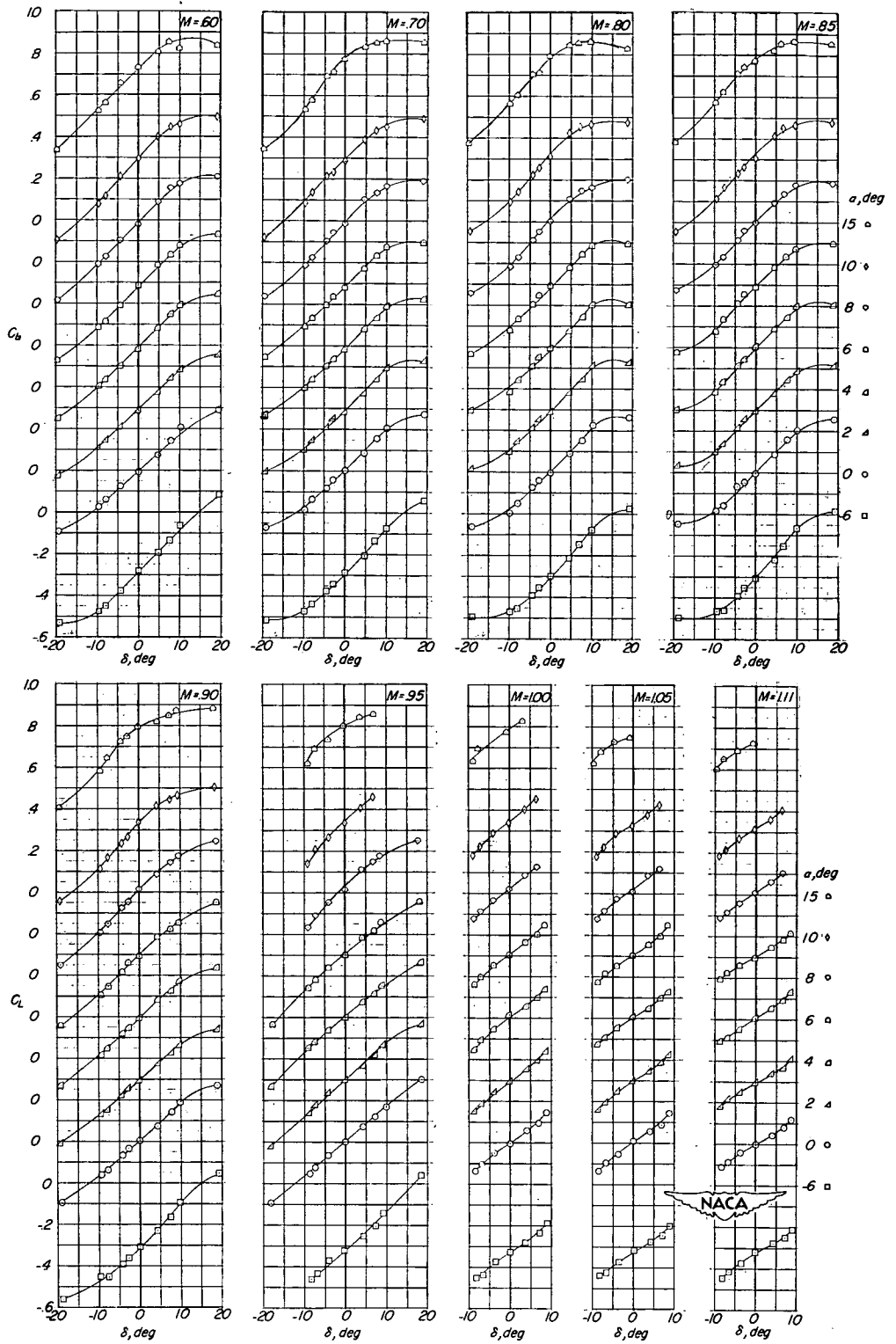


Figure 4.- Variation of lift coefficient with control deflection at various angles of attack for the single flap.

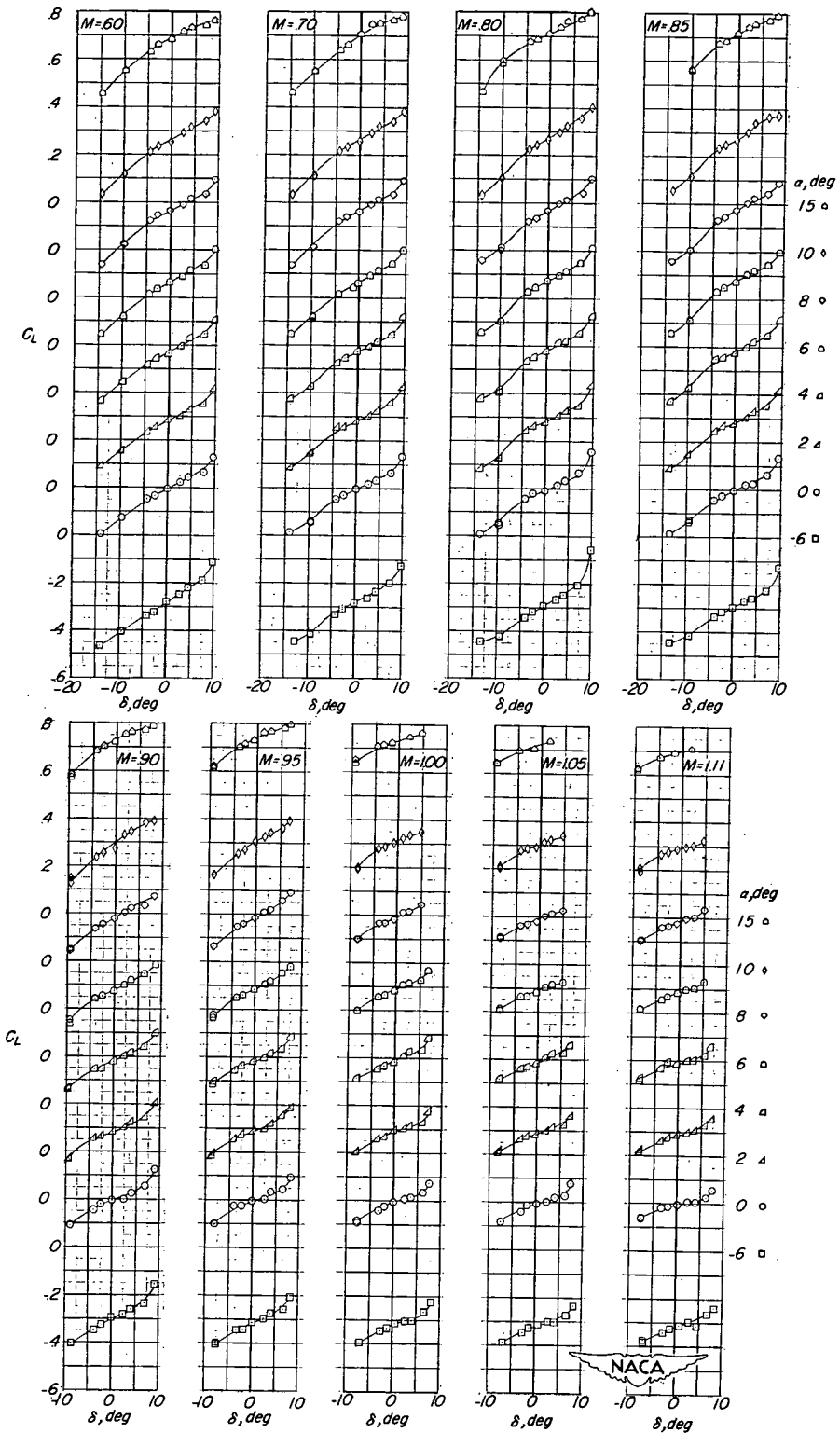


Figure 5.- Variation of lift coefficient with control deflection at various angles of attack for the tandem flap.

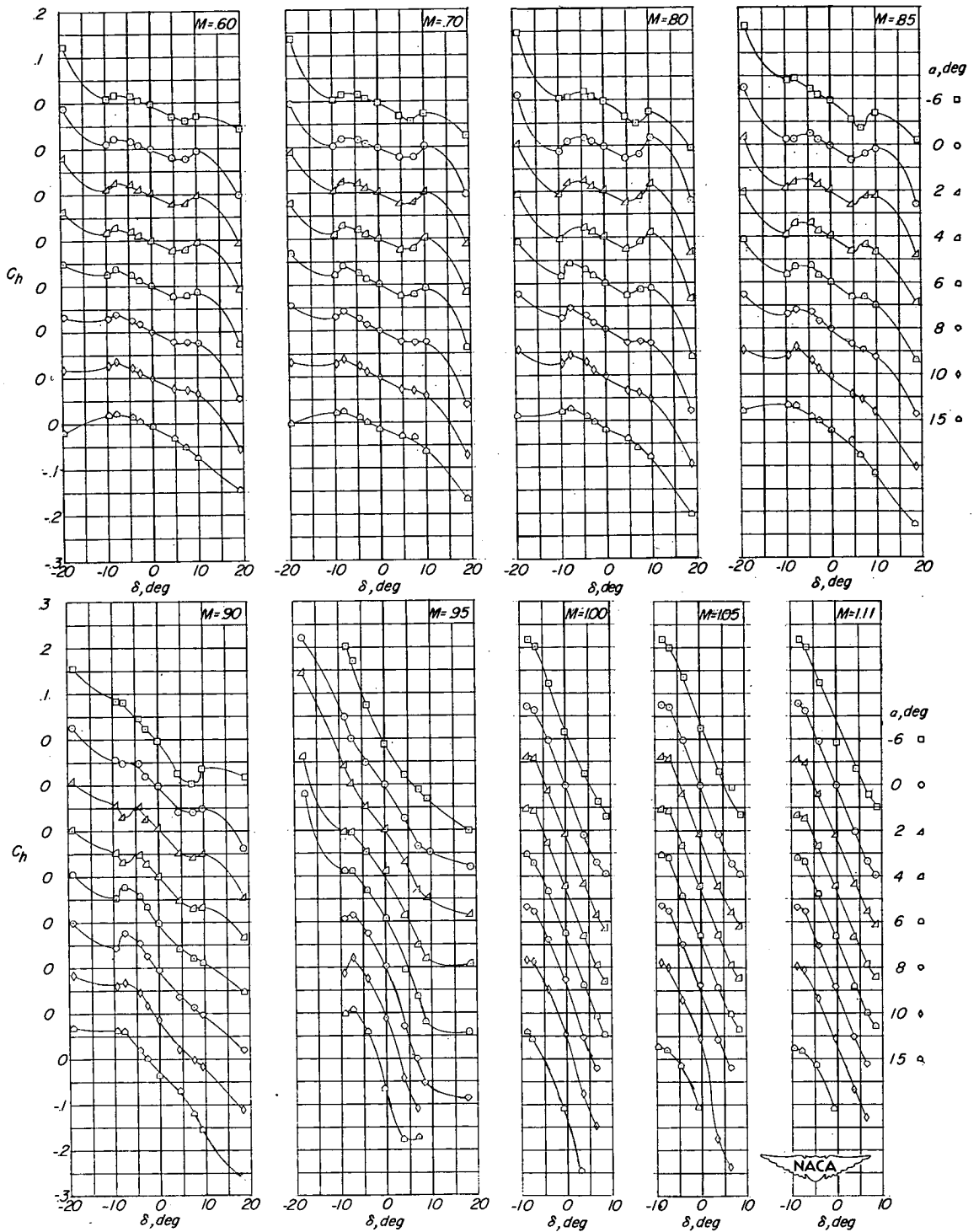


Figure 6.- Variation of hinge-moment coefficient with control deflection at various angles of attack for the single flap.

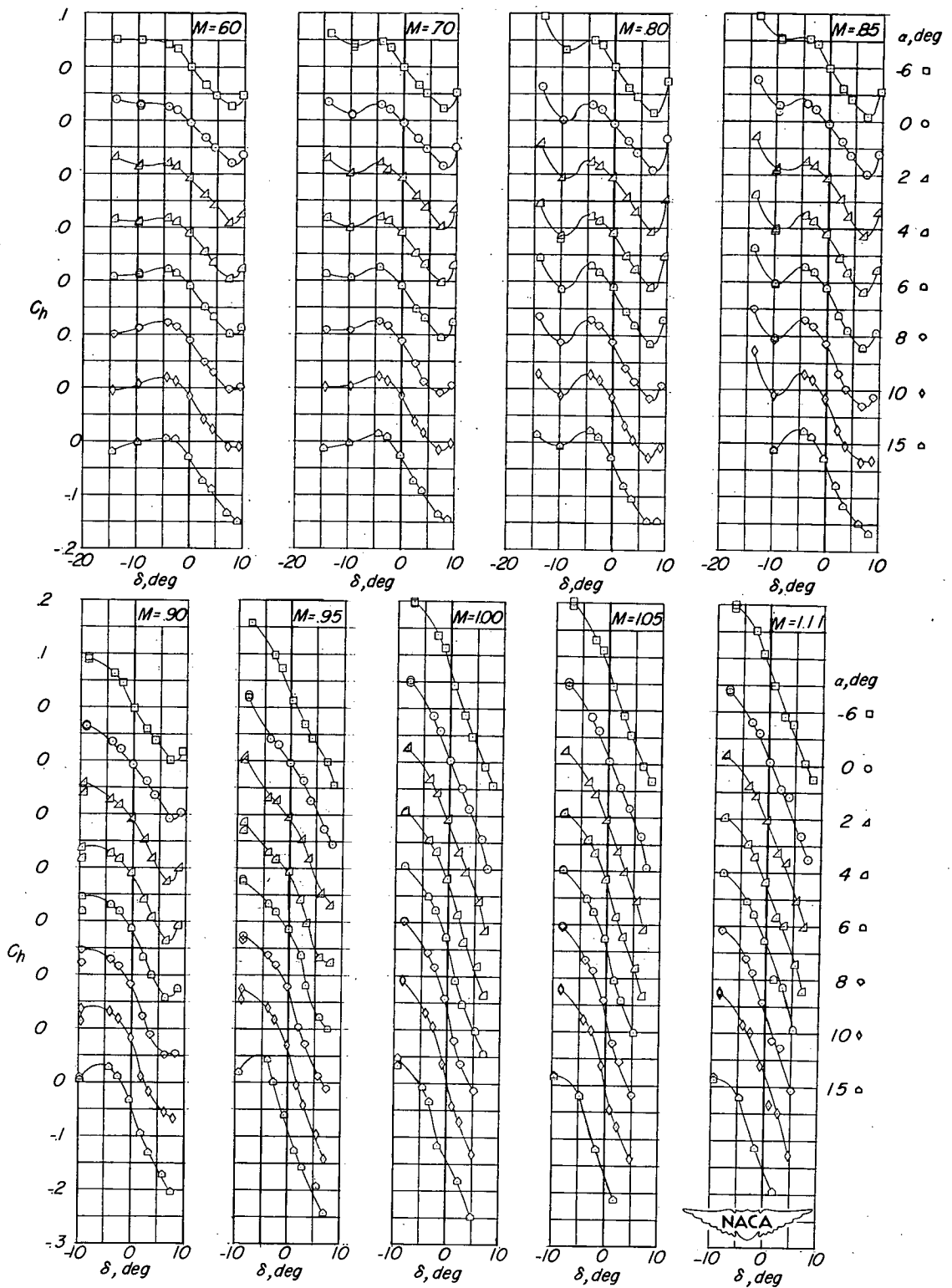


Figure 7.- Variation of hinge-moment coefficient with control deflection at various angles of attack for the tandem flap.

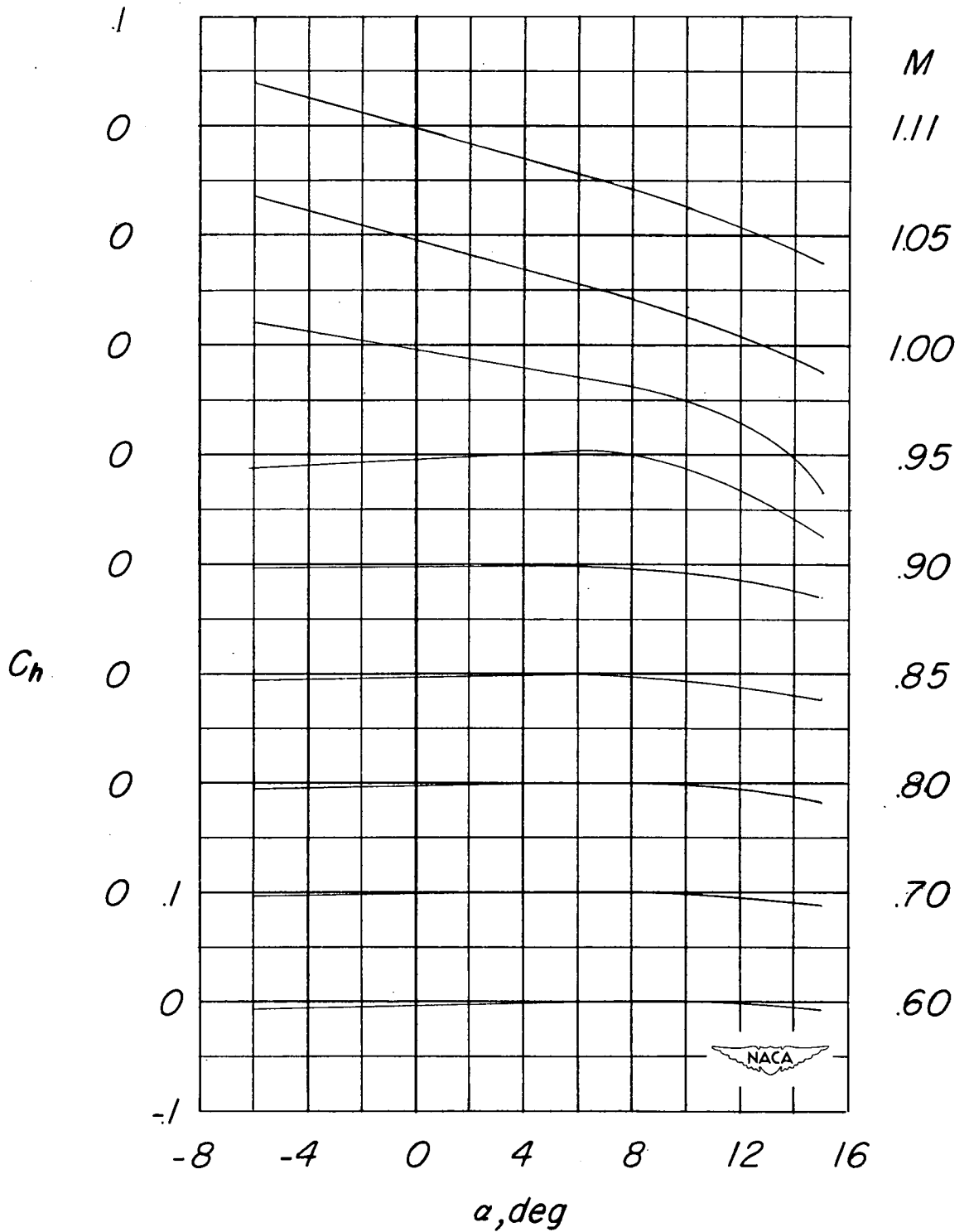


Figure 8.- Variation of hinge-moment coefficient with angle of attack at various Mach numbers for the single flap ($\delta = 0^\circ$).

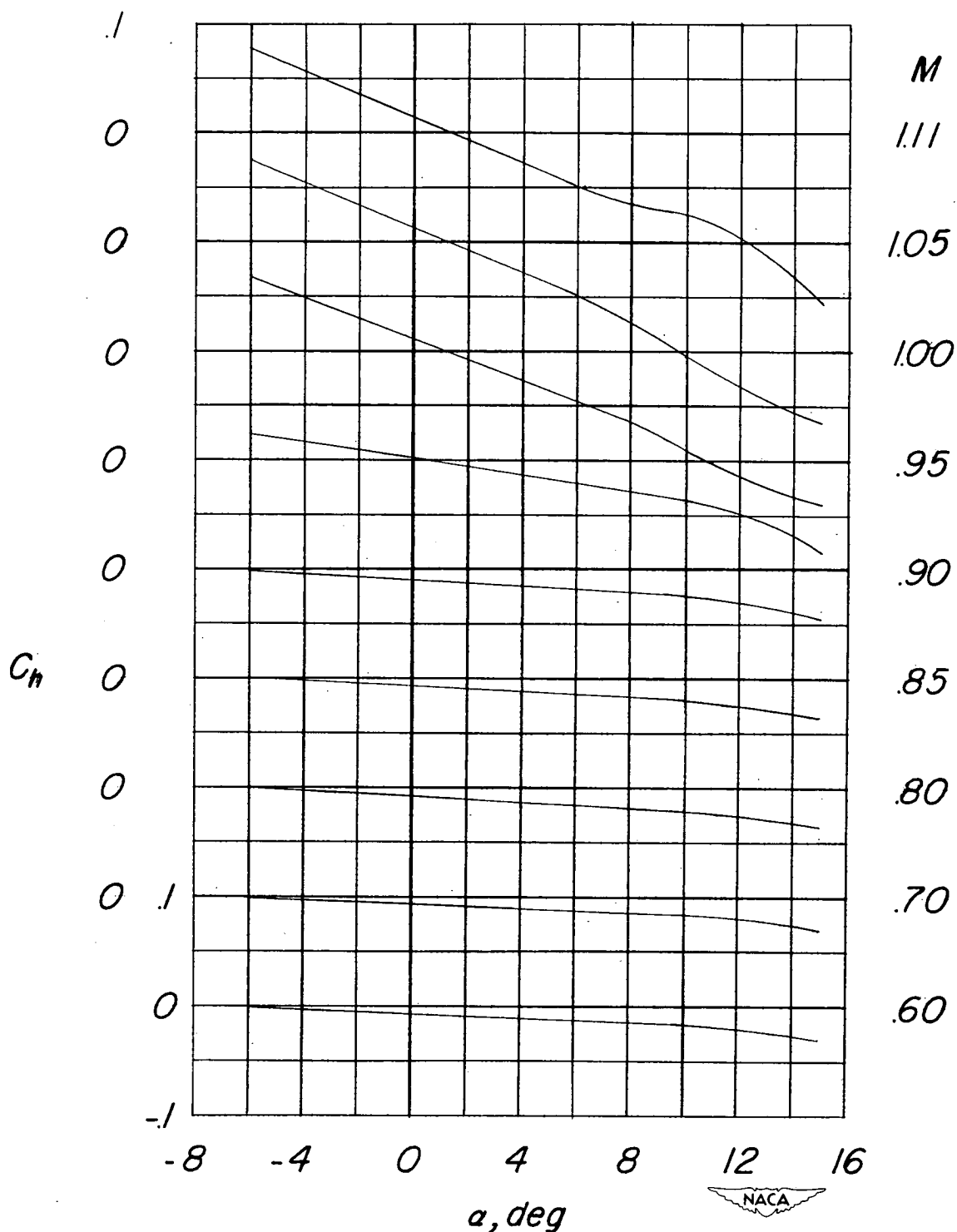


Figure 9.- Variation of hinge-moment coefficient with angle of attack at various Mach numbers for the tandem flap ($\delta = 0^\circ$).

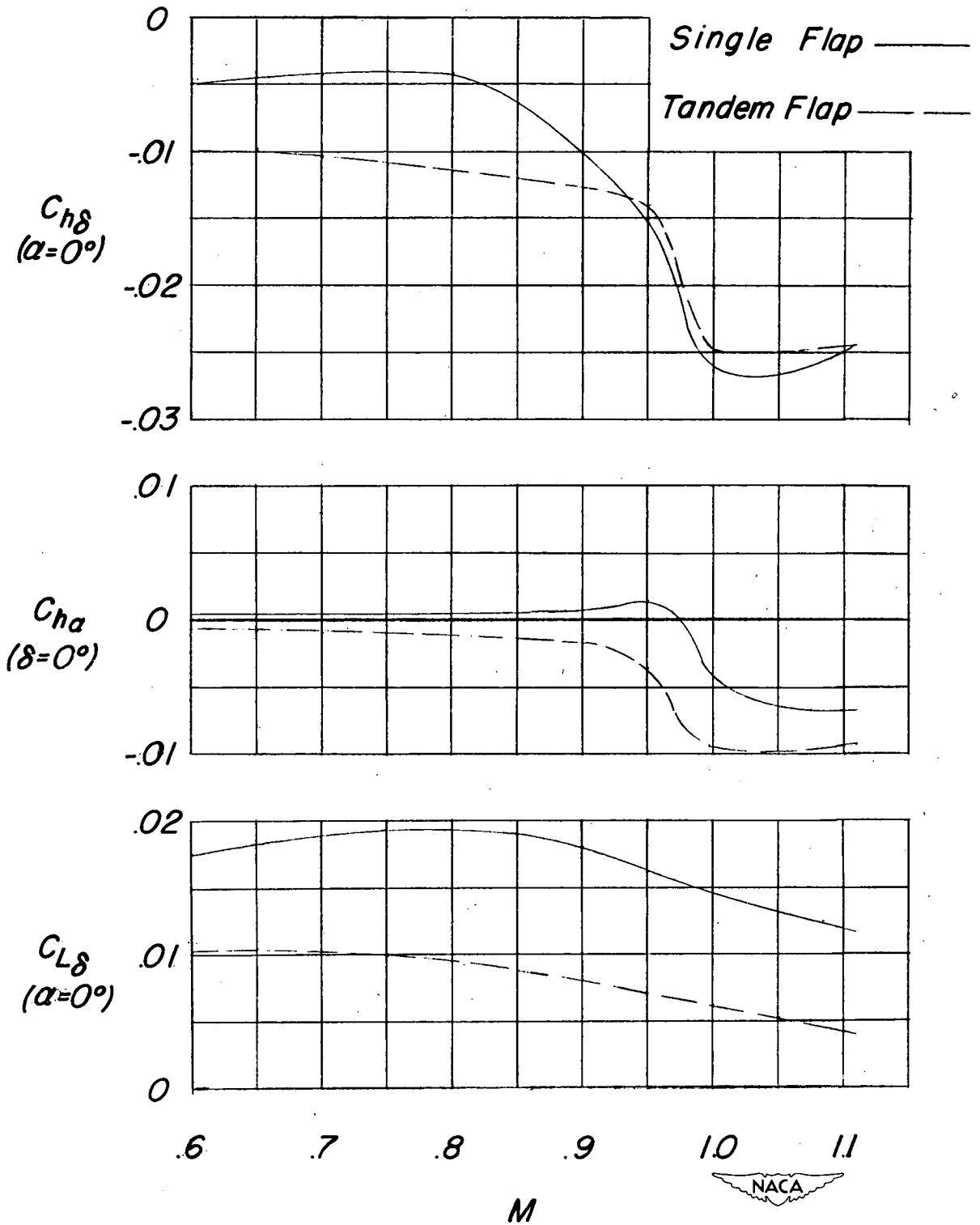


Figure 10.- Variation of the parameters $C_{h\delta}$, $C_{h\alpha}$, and $C_{L\delta}$ with Mach number for the single and tandem flaps.

